Condensation of isolated semi-flexible filaments driven by depletion interactions

A Letters Journal Exploring the Frontiers of Physics

August 2009

EPL, **87** (2009) 48006
doi: 10.1209/0295-5075/87/48006

www.epljournal.org

Condensation of isolated semi-flexible filaments driven by depletion interactions

A. W. C. Lau[1], A. Prasad[2] and Z. Dogic[3,4(a)]

[1] *Department of Physics, Florida Atlantic University - Boca Raton, FL 33431, USA*
[2] *Department of Chemical and Biological Engineering, Colorado State University - Fort Collins, CO 80523, USA*
[3] *Department of Physics, Brandeis University - Waltham, MA 02454, USA*
[4] *Rowland Institute at Harvard, Harvard University - Cambridge MA 02143, USA*

received 23 April 2009; accepted in final form 5 August 2009
published online 7 September 2009

PACS 82.70.Dd – Colloids
PACS 87.16.Ka – Filaments, microtubules, their networks, and supramolecular assemblies
PACS 82.35.Pq – Biopolymers, biopolymerization

Abstract – Using fluorescence microscopy, we directly visualize the condensed structures of individual semi-flexible actin filaments in a poor solvent. The condensation of filaments into either ring-like or racquet-like structures is driven by non-adsorbing polymers which induce attractive interactions between filaments via the well-known depletion mechanism. A quantitative analysis of the racquet structures yields a direct measurement of the adhesion strength between a pair of filaments. We also compare our experimental data with a theoretical model, demonstrating that in the limit of weak binding, thermal fluctuations can renormalize the effective strength of the attractive depletion interactions. Our experimental methods can be applied to other filamentous structures to directly measure their attractive intermolecular potentials.

Important structural and genomic components of a cell such as semiflexible actin filaments and DNA molecules are frequently found in highly condensed states [1]. These condensed structures, for example, appear in the cytoskeleton, wherein actin filaments form bundles to provide structural support for the cell [2], and in viral capsids [3,4] and chromosomes [5], wherein DNAs are tightly packed to provide an efficient information storage system. Many characteristics of these *in vivo* structures can be reproduced in simple *in vitro* systems [6–8]. For instance, upon addition of multivalent cations, DNA collapses into toroidal structures that bear striking similarity to assemblages found in virial capsids [7,9]. Therefore, with powerful experimental methods one can probe the structures of condensed semi-flexible polymers in simple *in vitro* systems to gain important insights into their biological functions. In addition to their biological significance, assemblages of highly condensed filaments, such as carbon nanotubes, play an important role for the design of new nanomaterials [10,11]. In this paper, we directly visualize the condensed structures of isolated actin filaments and extract valuable information about the nature of the attractive interactions between these filaments.

The conformational states of a polymer are highly dependent on the nature of the monomer-solvent interaction, *i.e.*, the solvent quality. In a good solvent, an isolated polymer assumes an entropy maximizing expanded coil state, whereas in a poor solvent, the polymer collapses into an energy minimizing condensed globule state [12]. At a critical solvent quality, the polymer undergoes a coil-globule transition [13]. While it has been well studied for flexible polymers, the nature of the coil-globule transition for semi-flexible polymers remains poorly understood. In particular, the structures of the semi-flexible polymers in the globule state are made complicated by the fact that they are not determined solely by the competition between entropy and monomer-solvent interaction, as in the case for flexible polymers, but also controlled by an additional elastic energy arising from backbone rigidity.

Previous theoretical [14–17] and experimental [7,10,11,18,19] work mainly focused on predicting and observing a variety of equilibrium structures, *e.g.*, rings, racquets, bundles and helices that are observed once attractive interactions induce the collapse of semi-flexible filaments. In addition, the mechanical properties

(a) E-mail: zdogic@brandeis.edu

of the resulting filament bundles have been recently measured [20,21]. In comparison, there have been very few direct and quantitative measurements of the attractive interaction between an isolated pair of filaments that drives these condensation transition in the first place. The most notable experimental measurements of this kind were carried out by Persegian and coworkers using the osmotic stress technique [22–24], where the average separation between filaments in a bundle is measured as a function of applied osmotic stress. Note, however, that even with this technique, one does not measure the true intermolecular interaction at the pair level but the response of the entire assemblage on the applied force.

Here, we describe an experimental technique that enables one to directly measure the average strength and the curvature of the adhesive potential between a pair of aligned semi-flexible actin filaments. This is accomplished by quantitatively analyzing the shape of isolated actin filaments in their condensed states. The condensation transition is driven by addition of non-adsorbing flexible polymers coils to a dilute suspension of actin filaments. Polymer coils induce attractive interactions between actin filaments via the well-known depletion mechanism [25]. Briefly, as two filament segments approach each other in the polymer suspension, an additional free volume becomes available to polymer coils, thus increasing the overall entropy of the mixture. The consequence is that of an effective attractive (depletion) potential between segments of the same actin filament. A particularly appealing feature of the depletion attraction is that the strength and the range of the attractive potential can be easily tuned by changing the polymer (depletant) concentration and their molecular weights [26]. Note that the strength of the depletion interaction scales linearly with the depletant concentration in the limit of dilute depletant concentration.

We use fluorescence microscopy to directly observe the formation and subsequent dynamics of the condensed structures —either rings or "racquets". A simple theoretical model, which includes thermal fluctuations of the filaments, in conjunction with quantitative image analysis allow us to extract the value of the adhesion strength between a pair of filaments. It has been commonly assumed that their fluctuations do not significantly influence the intermolecular potential, since actin filaments have a large persistence length of 17 μm. However, our data indicates that in the limit of low depletant concentration (or weak adhesion strength), the lateral fluctuations of the filaments renormalize the strength of the attractive interaction between two semiflexible filaments. We believe that our approach is the most direct measurements of the microscopic depletion interactions between a pair of semi-flexible filaments, and our results should complement recent works on macroscopic bundling transitions and bundle mechanics of semiflexible polymers [20,27,28].

Monomeric G-actin was isolated from frozen chicken skeletal muscle (Pel-Freeze) following the standard protocol and subsequently purified on a size exclusion column (Sephacryl S-200HR, GE Healthcare) [29,30]. Filamentous F-actin was polymerized in high ionic strength buffer and labeled with Alexa-488-phalloidin (Molecular Probes) at an equimolar dye to monomer ratio [31]. All samples were prepared in an AB buffer (30% sucrose w/w, 20 mM phosphate *p*H 7.5, 350 mM KCl, 0.5% mercaptoethanol, 3 mg/ml glucose, 20 μg/ml glucose oxidase, and 3.5 μg/ml catalase). Sucrose was added to slow down the desorption of Alexa-488-phalloidin from actin filaments. To obtain quasi 2D chambers, actin was confined between two No 1.5 coverslips, cleaned in a 0.5% solution of Hellmanex (Hellma Cells, PlainView NY) at 80 °C. Roughly, one-third of the samples had thickness of less than a micron, thin enough so that filaments remained in focus during the entire experiment. The concentration of actin filaments in the final sample is approximately 50 nM, which results in less than one filament per field of view and greatly reduces the probability of multi-filament condensates. As a depletant, we used either Poly(ethylene glycol) (PEG, MW 20000, Fluka) or Dextran (MW 500000, Fluka). For PEG samples, actin filaments did not absorb onto a confining glass surface, presumably due to the absorption of PEG onto a glass surface. For Dextran samples, actin filaments absorbed onto untreated coverslips due to the depletion effect. This absorption was suppressed by coating the surfaces with a polyacrylamide brush: Cleaned coverslips were first reacted with 3-(Trimethoxysilyl) propyl methacrylate (Sigma-Alrich) and subsequently with an aqueous solution containing 3% acrylamide, 0.07% ammonium persulfate, and 0.035% N, N, N′, N′-Tetramethylethylenediamine. The filaments were imaged with an inverted microscope (Nikon TE2000-U) equipped with a PlanFluor lens (100×, 1.3 NA) and 100 W mercury illumination. Time-lapse sequences of up to five hundred images, one second apart, were acquired using a cooled CCD camera (CoolSnap HQ, Roper Scientific). The sizes of the condensed structures, *e.g.* the circumferences of the racquet heads, were measured with the aid of an image processing code written in the IDL programming language. For each depletant concentration, we repeated the analysis from anywhere between 5 to 10 different racquets.

The capability to directly observe freely fluctuating filaments is essential for our experiments. A number of other studies have examined the structures of condensed filaments [7,32]. However, in these studies the condensed filament is usually absorbed onto a hard wall. A potential drawback of these experiments is that the filament-wall interaction could affect the nature of filament-filament interaction and thus the structure of the final condensate. In addition, absorbed filaments are stuck in a particular state, which does not exhibit any fluctuations, and they are thus unable to relax towards an equilibrium state. In contrast, our experimental methods developed in this paper allow one to observe the condensed structures

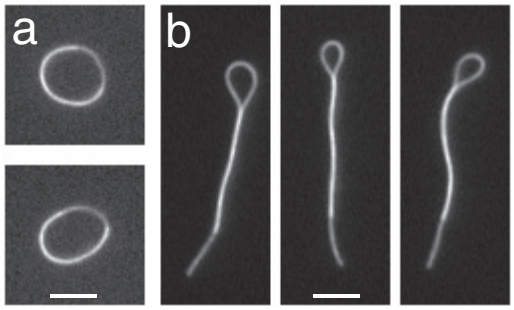

Fig. 1: Images of single actin filaments condensed into tori (a) and racquet conformations (b). The brightness along the handle part of the racquet is exactly twice the brightness of the filament in the racquet head which indicates that these condensate are formed from a single filament. PEG concentration is 1.65%. Scale bars are 3 μm.

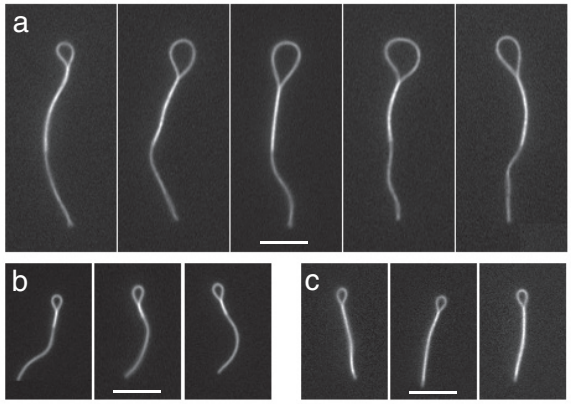

Fig. 2: Fluctuations of an actin racquet formed at a PEG concentration of 1.54% w/w (a), 2.3% w/w (b) and (c). Low polymer concentration leads to weak attractive interactions which result in large racquet heads (a). Strong attractions result in smaller racquet heads (b), (c). A comparison of images in (b) and (c) illustrates that the filament overlap in the racquet handles does not affect the size of the racquet head. All scale bars are 5 μm.

that are freely fluctuating while confined to quasi-2D chambers. We have compared the conformations of absorbed filaments to those that are freely fluctuating, and we found significant differences between these two cases. For these reasons, we believe that only freely fluctuating condensates can be described by an equilibrium theory and in this paper we only analyze these structures.

At low actin concentration, the probability of forming a multifilament condensate is very low, since filaments are well separated. However, even isolated filaments experience intramolecular attractions of sufficient strength to condense an entire filament into a compact structure. We observe single actin filaments condensed into either rings or racquets (see fig. 1). We can unambiguously confirm that these are indeed single filament condensates by quantitatively analyzing the intensity along the contour length of the filament. For example, in fig. 1(b), the intensity of the racquet handle is exactly twice the intensity of racquet head. The structure of the final condensed state depends on the kinetics: If the two ends of a filament initially bind each other in antiparallel fashion, a ring-like structure is formed (see fig. 1(a)). Once the ring is formed, we might expect that its radius would decrease as the filaments slide against each other. In principle, this process should continue until the ring reaches the minimum energy state, in which the adhesion energy, which favors a smaller ring, balances the bending energy which favors a larger ring. However, over a period of few hours, the radii of the rings remain unchanged and we observe a broad distribution of ring sizes. This suggests that the friction coefficient associated with filaments sliding within the bundle is large and that depletion induced actin bundles are not able to reach a global minimum but are rather kinetically trapped in a local minima, *i.e.* a metastable state. For these reasons a quantitative analysis of ring structures with an equilibrium theory of their morphologies is meaningless.

If the ends of a filament initially approach each other in a parallel fashion, the final condensate assumes a racquet-like structure (see figs. 1(b) and 2). After initial contact, the two parts of the filament bind each other until the force arising from the depletion attractions is balanced by the repulsive force arising from the elastic distortions of the racquet head. This "zipping up" is a fast process which does not involve any filament sliding. Once the racquet reaches this quasi-equilibrium state, in principle, it should slowly equilibrate on a longer time scale by sliding the filament segments against each other in order to maximize the filament overlap in a racquet handle. As in the case of the ring formation above, we do not observe this secondary process on our experimental time scales. However, in contrast to ring-like condensates, the sliding motion of the filaments in the handle part of the racquet does not affect the size of the racquet head, as illustrated in fig. 2. Indeed, we observe that within each sample the size of all racquet heads are approximately the same and independent of the filament overlap in the racquet handle. For this reasons we quantitatively analyze the condensed state in which isolated actin polymers assume a shape of racquets.

Increasing the depletant concentration leads to a stronger attraction, and thereby results in smaller racquet heads (fig. 2). The measurements of the racquet head size as a function of concentration of PEG and Dextran are shown in fig. 3. As expected, we observe large racquet heads at low polymer concentration (weak adhesion potential) and small heads at high polymer concentrations (strong adhesion potentials). Both PEG and Dextran data exhibit the same qualitative features. Indeed, if the polymer concentrations are rescaled by a constant, both PEG and Dextran data lie on top of each other (see inset of fig. 3), indicating a universal effect which is independent of the details of the depleting polymer.

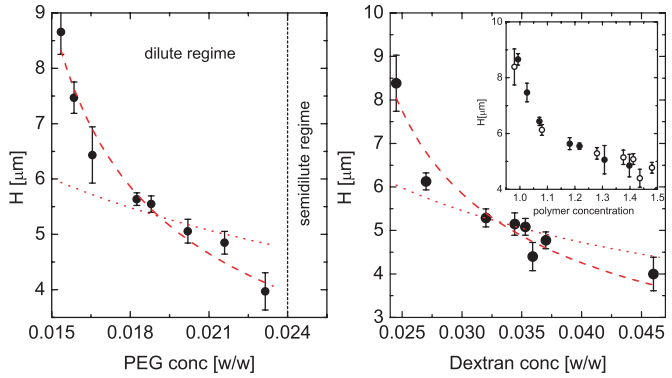

Fig. 3: (Colour on-line) The circumference of the actin racquet H plotted as a function of PEG concentration (left) and Dextran concentration (right). The dotted line corresponds to the model which neglects thermal fluctuations and the dashed lines corresponds the model which takes into account thermal fluctuations. Inset: The two sets of data lie on top of each other if the concentrations of Dextran and PEG are rescaled.

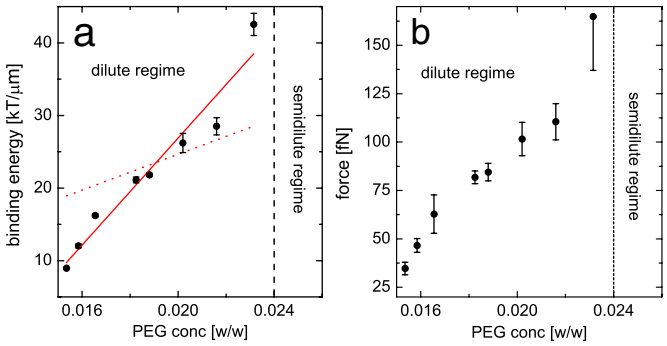

Fig. 4: (Colour on-line) (a) The adhesion strength calculated from the relationship, $H^2 = 36.662\,\kappa/\lambda$, is plotted as a function of PEG concentration. The dotted line corresponds to the case where adhesion strength scales linearly with polymer concentration. The dashed line corresponds to a theory that takes thermal fluctuations of the filaments into account. (b) The measurements of the force exerted on a semi-flexible filament when it is bent into racquet-like shape, plotted as a function of depletant concentration.

In order to quantitatively relate the structures of the racquet to the strength of the adhesion interaction, we follow the model of ref. [15], and decompose a racquet into a ring with circumference H and two "attached" parallel rods (the handle). The elastic energy of a racquet head can be calculated by treating the filament as a thin isotropic rod, *i.e.* as an Euler elastica, described by a differential equation for the structure, $\kappa\,\mathrm{d}^2\theta(s)/\mathrm{d}s^2 + F\sin\theta = 0$, where $\theta(s)$ is the local tangent as a function of the contour position s, F is the force required to clamp down the two ends of the filament at the racquet base [33], and κ is the bending modulus of the actin. Solving the differential equation with appropriate boundary conditions yields the elastic energy stored in the racquet head $E_{el} = 18.331\kappa/H$ [16], where $\kappa = 17\,k_BT\,\mu$m for an actin filament [31]. It follows that the total energy of an actin racquet can be written as a sum of the elastic energy of the ring and the adhesion energy of the handle: $E_{\mathrm{tot}} = 18.331\,\kappa/H - \lambda\,(L-H)/2$, where λ is the adhesion energy per unit length and L is the contour length of the entire filament. The equilibrium value of H is obtained by minimizing the total energy of a racquet: $H_{\mathrm{eq}}^2 = 36.662\,\kappa/\lambda$. This relation can be used to measure the binding energy between two filaments, λ_{exp}, which is of the order of tens of k_BT per micron (see fig. 4(a)). In addition to measuring the adhesion strength, we can also estimate the force required to deform the filaments into a racquet according to $F = 39.65\,\kappa/H^2$. Using this method, we measure forces as low as 25 fN's, as shown in fig. 4(b).

Next, we relate the equilibrium circumference H_{eq} to the polymer concentration. Within the Asakura-Oosawa model of the depletion interaction, we expect that the adhesion energy varies linearly with depletant volume fraction ($\lambda_{\mathrm{dir}} \sim \phi_{\mathrm{p}}$). It follows that $H_{\mathrm{eq}} \sim 1/\sqrt{\phi}_{\mathrm{p}}$. As can be seen in fig. 3, this simple model fails to describe quantitatively our experimental data, especially in the limit of low ϕ_{p}. There might be a few reasons for this discrepancy. It is plausible that the highly curved actin racquets are no longer described by linear elasticity, or that depleting polymer can no longer be treated as ideal interpenetrating spheres so that λ_{dir} is no longer linearly proportional to the concentration. However, if either of these effects were important, we expect that the deviations from linear behaviors occur in the limit of small actin racquets (large curvatures) or equivalently high depletant concentrations. Another possibility is that visualized racquets are not perfectly confined to the image plane. This would disproportionately affect the analysis of smaller racquets. Since we only analyze images in which the entire racquet lies in focus, the upper bound on motion of racquets in the z-direction is about $0.5\,\mu$m. Even for the smallest structures analyzed here, the fluctuations in the z-direction would reduce the measured racquet size by at most 5%, which does not account for the discrepancy between theory and experiment in fig. 3(a).

A more compelling reason for the discrepancy between the simple theory and our experiments comes from the effect of the filament fluctuations [34]. As the adhesion strength decreases, the fluctuations of two semi-flexible filaments in the handle of the racquet about their equilibrium separations becomes significant, and we expect that this effect will contribute to the free energy. Here, we propose a simple quantitative model which accounts for entropic fluctuations of filaments. For simplicity, we take the fluctuations of a racquets to be that of the fluctuations of the ring part plus the fluctuation corrections in the handle part of the racquet, assuming that they are additive. The fluctuation contribution to the free energy of a semiflexible ring can be computed following the formulation of ref. [35]. The Hamiltonian for the ring is $\mathcal{H}_{\mathrm{ring}} = (\kappa/2)\int_0^H (\mathrm{d}\delta\phi/\mathrm{d}s)^2$, where $\delta\phi(s)$ is the small

deviation of the azimuthal angle from a perfect circular ring: $\phi_0(s) = 2\pi s/H$ and s is the arclength. Expanding $\delta\phi(s) = \sum_{n=2}^{\infty} \delta\phi_n \cos(2\pi n s/H)$ and subtracting out the fluctuation correction of a short semiflexible filament, we find $\Delta F_{\rm ring} \approx -k_B T \ln(H/\ell_p)$, where ℓ_p is the persistence length. Thus, the fluctuations of the ring contribute a logarithmic correction to the free energy, and we expect it to be subdominant compared to the elastic energy since the radii of the ring in our experiments are small compared to the persistence length of actin. Thus, in our theoretical analysis below, we assumed this contribution to be negligible, and we only take into account the fluctuation corrections in the handle part of the racquet, which is modeled by the two semiflexible rods with an attractive potential. The Hamiltonian is

$$\mathcal{H} = \sum_i \frac{\kappa}{2} \int_0^{L_H} \mathrm{d}s \left(\frac{\partial^2 \mathbf{r}_i(s)}{\partial s^2} \right)^2 + \int_0^{L_H} \mathrm{d}s \int_0^{L_H} \mathrm{d}s'\, V(|\mathbf{r}_1(s) - \mathbf{r}_2(s')|), \qquad (1)$$

where $\mathbf{r}_i(s)$ describes the contour of the polymer i, s is the arclength, κ is the bending rigidity, L_H is the length of the filaments in the handle, and $V(x)$ is the interaction potential between the polymers. Note that $\lambda_{\rm dir} \equiv |V(r^*)|$, where r^* is the equilibrium distance. To get the fluctuation contribution, we look at $\delta\mathbf{r}(s) \equiv \frac{1}{2}[\delta\mathbf{r}_1(s) - \delta\mathbf{r}_2(s)]$, where $\delta\mathbf{r}_i(s) = [\delta r_{ix}(s), \delta r_{iy}(s), 0]$ is the deviation of the i-th polymer from the straight line configuration. Within the harmonic approximation, the fluctuation term can be evaluated as[1]

$$\frac{\Delta F}{L_H} = \frac{k_B T}{2} \int_{-\infty}^{\infty} \frac{\mathrm{d}q}{2\pi} \ln\left(\frac{\alpha + \kappa\, q^4}{\kappa\, q^4} \right) = \frac{k_B T}{\sqrt{2}} \left(\frac{\alpha}{\kappa} \right)^{1/4}, \quad (2)$$

where we have subtracted out the infinite part corresponding to the fluctuations of a free polymer, and $\alpha \equiv V''(r^*)$, *i.e.*, the second derivative of the interaction potential evaluated at the equilibrium distance r^* [24]. Note that the fluctuation contribution decreases with increasing bending rigidity, as expected. Therefore, we can write the free energy of the handle part of the racquet as $F_H \simeq \lambda^*(L - H)$, where the renormalized adhesion strength is defined as $\lambda^* \equiv \lambda_{\rm dir} - k_b T\,[\alpha/(4\kappa)]^{1/4}$. Minimizing the total free energy of a racquet, we find $H^2 = 36.662\,\kappa/\lambda^*$. In contrast to the previous case, the effective λ^* decreases more drastically due to the fluctuations, thus giving rise to a larger ring size, consistent with our experimental observations. Next, we fit our experimental data with the following formula:

$$H^2 = \frac{A}{\phi_{\rm p}^{1/4}(\phi_{\rm p}^{3/4} - B)}, \qquad (3)$$

where $A \equiv 36.6\,\kappa\,\phi_{\rm p}/\lambda_{\rm dir}$ and $B \equiv k_B T(\phi_{\rm p}^{3/4}/\lambda_{\rm dir}) \times (\alpha/4\,\kappa)^{1/4}$. Note that in deriving eq. (3), we have assumed that both $\lambda_{\rm dir}$ and α are linearly proportional to $\phi_{\rm p}$. As can be seen in fig. 3, this model fits our data very well with the best-fit parameters given by $A = 0.13\,\mu\mathrm{m}^2$ and $B = 0.038$ for the PEG case. It is interesting to estimate the average squared fluctuation length: $d_0^2 \equiv (1/L_H)\int_0^{L_H} \mathrm{d}s\, \langle \delta\mathbf{r}^2(s) \rangle = (\pi k_B T/\alpha)(\alpha/4\kappa)^{1/4} = (\pi/4) \times (k_B T/\kappa)^4 (1/\phi^{3/4})(A/40B)^3$. For a lower polymer concentration of 0.015, we obtain the value of $d_0 \sim 0.6\,\mathrm{nm}$. It is encouraging that by analyzing micron sized structures we can estimate lateral fluctuations that have the right order of magnitude. It is also important to note that the magnitude of lateral fluctuations is significantly smaller then the range of the attractive potential which is of the order of 10 nm. This indicates that two filaments almost always stay bound to each other and thus justifies our theoretical approximation.

Next, we estimate the shape of the intermolecular potential between two filaments and from the shape of this potential we independently extract the values of parameters A and B. We show that these values are in reasonable agreement with the values of parameters A and B obtained by analyzing structure of mesoscopic condensates in fig. 3(a). Note, that A is directly related to the depth of the attractive minimum while B is proportional to the curvature of the potential at its minimum. The interaction potential between two parallel filaments is described as $V(r) = k_B T(\ell_B/b^2) K_0(r/\lambda_S) + V_{\rm d}(r)$, where r is the distance between the filaments. The first term represents the screened Coulomb interaction between two charged rods with $\ell_B \equiv e^2/\epsilon k_B T \sim 7\,\text{Å}$ is the Bjeerum length in water, b is the average distance per charge, $K_0(x)$ is the zeroth-order Bessel function of the second kind, and λ_S is the Debye screening length. The second term is the well-known depletion interaction given by

$$V_{\rm d}(r) = 2k_B T c_{\rm p} \left[r\sqrt{d^2 - r^2} - d^2 \tan^{-1}\left(\frac{\sqrt{d^2 - r^2}}{r} \right) \right],$$

where $c_{\rm p}$ is the concentration of the polymers, $d = a + R_G$, a is the radius of an actin filament, and R_G is the radius of gyration of the flexible polymers. The term in the bracket represents the excluded volume of two rods in the presence of small spherical particles. We numerically solve for the equilibrium distance r^* at which $\mathrm{d}V(r)/\mathrm{d}r = 0$, and evaluate $\lambda_{\rm dir} = |V(r^*)|$ and $\alpha = \mathrm{d}^2 V(r)/\mathrm{d}r^2|_{r=r^*}$. As a consistency check, we have verified that both $\lambda_{\rm dir}$ and α scale roughly linearly with the number concentration $c_{\rm p}$ for the range of concentrations of flexible polymer carried out in our experiments. Estimating the relevant parameters in our experiments ($b \sim \ell_B$, $\lambda_S \sim 0.5\,\mathrm{nm}$, $a \sim 4\,\mathrm{nm}$, $R_G \sim 7\,\mathrm{nm}$) we find that $r^* \sim 5\,\mathrm{nm}$, $A \sim 0.1\,\mu\mathrm{m}^2$, and $B \sim 0.02$. These estimates are in reasonable agreement with the values of A and B obtain by fitting data in fig. 3 thus providing an independent confirmation that our theoretical model captures the essential physics of actin filaments condensed into racquets structure.

[1] Strictly speaking, we should use a discrete sum. However, the continuum approximation used here should be valid for long polymers.

In conclusion, by analyzing the structure of semi-flexible filaments collapsed into racquet-like structures, we directly measure the strength of the attractive potential that drives the condensation of these filaments. Using this method we characterize the depletion induced attractive potential between a pair of actin filaments. Depletion interactions, which arise whenever small non-adsorbing polymer are added to colloidal particles of any shape, are of great importance in soft matter physics, and are capable of driving a variety of self-assembly processes for both spherical and filamentous colloids [36–38]. For micron sized colloidal spheres, the shape of the depletion potentials has been fully characterized using line scanning optical tweezer setup [36]. In contrast, measuring the full characteristics of the depletion potential between 7 nm thick actin filaments is a more difficult task, due to smaller length scales involved. Analysis of condensed actin filaments in a racquet-like structures yields the depth of the depletion potential and the curvature of the depletion potential at its minimum. The values we obtain are in agreement with the standard Asakura-Oosawa picture of depletion potential. Additionally, we show that in the limit of weak adhesion strength filament's fluctuations renormalize direct intermolecular interactions, even for actin filaments which have a fairly large persistence length. The experimental methods described in this paper are very general and can be used to analyze the attractive interactions for other filamentous structures, such as viruses, DNA, and microtubules. They can also be used to analyze cases where filament condensation is driven by other mechanisms such as multivalent cations or van der Waals interactions.

* * *

This work was supported by Rowland Institute at Harvard and NSF through grants DMR-0705855 (ZD), DMR-MRSEC-0820492 (ZD), and DMR-0701610 (AWCL). We thank T. C. Lubensky and J. Kondev for helpful discussions, and E. Barry for his help with the image analysis.

REFERENCES

[1] Alberts B. *et al.*, *Molecular Biology of the Cell* (Garland, New York) 2008.
[2] Furukawa R. and Fechheimer M., *Int. Rev. Cytol.*, **175** (1997) 29.
[3] Purohit P. K. *et al.*, *Proc. Natl. Acad. Sci. U.S.A.*, **100** (2003) 3173.
[4] Rudnick J. and Bruinsma R., *Phys. Rev. Lett.*, **94** (2005) 038101.
[5] Schiessel H., *J. Phys.: Condens. Matter*, **15** (2003) R699.
[6] Tang J. X. *et al.*, *Biochemistry*, **36** (1997) 12600.
[7] Bloomfield V. A., *Biopolymers*, **31** (1991) 1471.
[8] Wong. G. C. L., *Curr. Opin. Colloid Interfrace Sci.*, **11** (2006) 310.
[9] Hud N. V. and Downing K. H., *Proc. Natl. Acad. Sci. U.S.A.*, **98** (2001) 14925.
[10] Terrones M. *et al.*, *Nature*, **388** (1997) 52.
[11] Martel R. *et al.*, *Nature*, **398** (1999) 299.
[12] de Gennes P. G., *Scaling Concepts in Polymer Physics* (Cornell University Press, Ithaca) 1979.
[13] Lifshitz I. M. *et al.*, *Rev. Mod. Phys.*, **50** (1978) 683; Nishio I. *et al.*, *Nature*, **281** (1979) 208.
[14] de Vries R., *Biophys. J.*, **80** (2001) 1186.
[15] Cohen A. E. and Mahadevan L., *Proc. Natl. Acad. Sci. U.S.A.*, **100** (2003) 12141.
[16] Schnurr B. *et al.*, *Europhys. Lett*, **51** (2000) 279; Schnurr B. *et al.*, *Phys. Rev. E*, **65** (2002) 061904.
[17] Snir Y. and Kamein R. D., *Science*, **307** (2005) 1067.
[18] Tang J. X. *et al.*, *Eur. Biophys. J.*, **30** (2001) 477.
[19] Hosek M. and Tang J. X., *Phys. Rev. E*, **69** (2004) 051907.
[20] Bathe M. *et al.*, *Biophys J.*, **94** (2008) 2955.
[21] Claessens M. M. A. E., Bathe M., Frey E. and Bausch A. R., *Nat. Mater.*, **5** (2006) 748.
[22] Podgornik R., Rau D. C. and Parsegian V. A., *Macromolecules*, **22** (1989) 1780.
[23] Rau D. C., Lee B. and Parsegian V. A., *Proc. Natl. Acad. Sci. U.S.A.*, **81** (1984) 2621.
[24] Strey H. H., Persegian V. A. and Podgornik R., *Phys. Rev. E*, **59** (1999) 999.
[25] Asakura S. and Oosawa F., *J. Polym. Sci.*, **33** (1958) 183.
[26] Lekkerkerker H. N. W., Poon W. C. K., Pusey P. N., Stroobants A. and Warren P. B., *Europhys. Lett.*, **20** (1992) 559.
[27] Heussingr C. *et al.*, *Phys. Rev. Lett.*, **99** (2007) 048101.
[28] Lieleg O. *et al.*, *Phys. Rev. Lett.*, **99** (2007) 088102.
[29] MacLean-Fletcher S. and Pollard T. D., *Biochem. Biophys. Res. Commun.*, **96** (1980) 18.
[30] Pardee J. D. and Spudich J. A., *Methods Enzymol.*, **85** (1982) 164.
[31] Brangwynne C. P. *et al.*, *Biophys. J*, **93** (2007) 346.
[32] Maurstad G. and Sokke B. T., *Curr. Opin. Colloid Interface Sci.*, **10** (2005) 16.
[33] Purohit P. and Nelson P. C., *Phys. Rev. E*, **74** (2006) 061907.
[34] Odijk T., *J. Chem. Phys.*, **108** (1998) 6923.
[35] Alim K. and Frey E., *Phys. Rev. Lett.*, **99** (2007) 198102; *Eur. Phys. J. E*, **24** (2007) 185.
[36] Yodh A. G. *et al.*, *Philos. Trans. R. Soc. A.*, **359** (921) 2001.
[37] Dogic Z. and Fraden S., *Philos. Trans. R. Soc. London, Ser A*, **359** (2001) 997.
[38] Crocker J. C., Matteo J. A., Dinsmore A. D. and Yodh A. G., *Phys. Rev. Lett.*, **82** (1999) 4352.